Fall 9-1-1983

The Far-Field Radiation Characteristics of a Resonant Conducting Ring on a Grounded Dielectric Substrate

R L. Holland
University of Colorado Boulder

Edward F. Kuester
University of Colorado Boulder

THE FAR-FIELD RADIATION CHARACTERISTICS OF A RESONANT CONDUCTING RING ON A GROUNDED DIELECTRIC SUBSTRATE

by

R. L. Holland and E. F. Kuester

Scientific Report No. 76

September 1983

Electromagnetics Laboratory
Dept. of Electrical and Computer Engineering
University of Colorado
Boulder, Colorado 80309

*This work was supported by the Office of Naval Research under Grant N00014-82-K-0264.

THE FAR-FIELD RADIATION CHARACTERISTICS OF A RESONANT CONDUCTING RING ON A GROUNDED DIELECTRIC SUBSTRATE

by

R. L. Holland and E. F. Kuester
Electromagnetics Laboratory
Dept. of Electrical and Computer Engineering
University of Colorado
Boulder, Colorado 80309

ABSTRACT

Interest in the use of curved microstrip sections over grounded substrates as compact, circularly polarized radiators for integrated microwave circuit applications has encouraged a variety of attempts to derive an adequate characterization of the far-field radiation of such elements. However, to this point these attempts have fallen into a category of microstrip radiation estimates which account for the presence of the substrate through the use of the low frequency equivalent width of the microstrip line. This report discusses an approach to this problem which proceeds from a determination of the Green's function appropriate for a conducting ring over a grounded substrate of arbitrary thickness and refractive index to integral representations of the electric and magnetic fields associated with this configuration. Successive stationary phase evaluations of the field integral representations for parameter values consistent with far-field conditions provides a single finite Poynting integral with a closed form integrand.

A power pattern analysis shows that the ring element over a grounded substrate is capable of significant broadside radiation in its lowest mode of resonance, but that it exhibits more exaggerated endfire behavior as the order of resonance increases.

Section 1. PROLOGUE

1.0 *Introduction*

Section 1 provides a discussion of the problem addressed in this report, its definition, history, and motivation, and then highlights the analytical approach employed in the solution of the problem. In addition, a summary of results and conclusions derived from the study reported here is given. The sections to follow present details of the solution procedure as well as a comparison of the results of this report with those of other authors addressing the same basic problem. The final section contains useful approximate solutions which are applicable for certain special instances of the more general circumstances for which a solution has been obtained.

1.1 *Problem Definition*

Interest in the use of microstrip annular-rings as integrated microwave circuit components capable of energy storage or radiation has inspired several studies whose objective it was to analytically characterize the behavior of such structures when they rest on a grounded dielectric substrate. Certain of these investigations have been more specifically directed toward a large class of applications wherein the electrical width of the circular-ring is small enough to justify neglecting any radially directed currents on the ring as well as any radial variation in longitudinal currents [1, 2]. It was the objective of this study to characterize the skywave radiated energy of such annular-rings, those for which the long-wavelength assumption is valid, by solving the relatively simple problem of a closed metallic ring over a grounded substrate. Specifically, it was desired that not only the total radiated power should be specified, but also that radiation power patterns be determined in order to more readily appraise the potential of these structures as antenna elements.

The basic physical configuration of interest in this report is illustrated in Figure 1.1-1. A circular, perfectly conducting ring of radius r_0 rests on top of a grounded dielectric substrate of thickness τ. The refractive index of the substrate is designated as n_2 and the ground plane is considered to be perfectly conducting. The refractive index of the medium above the substrate is taken to be 1, and the physical extent of the grounded substrate is infinite. For later reference, circular cylindrical and spherical coordinate reference systems are also depicted in Figure 1.1-1. The coordinate origin lies on the upper surface of the ground plane, a distance τ directly below the center of the conducting ring. The unit vectors of the cylindrical system are $\hat{r}$, $\hat{\varphi}$, $\hat{z}$, and those of the spherical system are $\hat{R}$, $\hat{\varphi}$, $\hat{\vartheta}$.

1.2 *Analytical Approach*

For analytical purposes, the conducting ring is considered equivalent to a traveling wave of current confined to a circular path of radius r_0. The circular cylindrical geometry and the absence of material boundaries in the radial direction for any given value of the z-coordinate allow Hankel transform integral representations for the Cartesian field components E_z and H_z. Of course, knowledge of these Cartesian field components (or their Hankel transforms) allows determination of the remaining field components, so one is justified in concentrating on E_z and H_z.

Since E_z and H_z satisfy the Helmholtz equation, the physical configuration of our problem leads to an inhomogeneous boundary value problem for the solution of the Hankel transforms $\tilde{E}_z$ and $\tilde{H}_z$ of E_z and H_z, respectively. Applying continuity conditions at both material interfaces and employing source conditions at the current ring, $\tilde{E}_z$ and $\tilde{H}_z$ are determined and, hence, integral representations are produced for all field components in terms of these Hankel

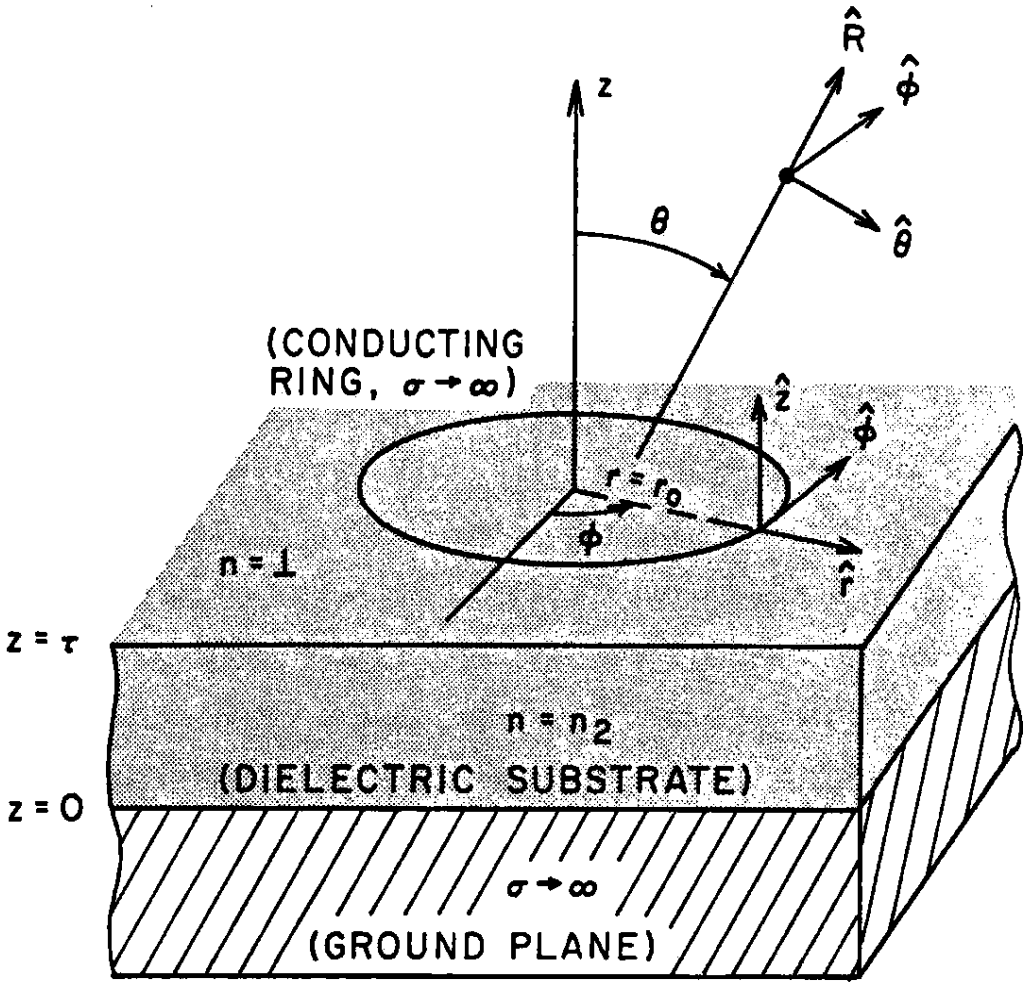

Fig. 1.1-1. The Physical Configuration of the Conducting Ring on a Grounded Substrate - A Cross-Sectional View

transforms.

Once integral representations for each of the field components are available, these are asymptotically evaluated to yield the far-field, skywave forms of each field component. Finally, the far-field forms of the electric and magnetic field components are employed to generate the far-field power density expressions and subsequently, via a Poynting integral, the total skywave radiated power.

1.3 *Summary of Results*

Following the analytical procedure outlined in Section 1.2 yields an expression for the total skywave radiated power in the form of a finite Poynting integral with a closed form integrand. Not only is the resultant expression readily evaluated numerically, it also permits the determination of useful approximate analytical forms which either do not involve an integral, or which include terms with integrals that are tabulated.

Consideration of the skywave power density expression associated with the Poynting power integral leads to the conclusion that the conducting ring configuration depicted in Figure 1.1-1 is capable of producing radiation along the z-axis only for the lowest order of resonance of the current on the ring. As the order of resonance increases, the skywave power density function exhibits a null along the z-axis and a direction of maximum absolute value that tends towards grazing incidence with the dielectric substrate (note the symmetry expected in the solution with respect to the φ - coordinate). In addition to launching radiation at increasingly larger angles from the zenith, the higher orders of resonance also exhibit successively reduced amounts of absolute power radiated, a result interpreted as manifesting increased confinement of the higher order modes by the ring structure.

Section 2. SOLUTION OUTLINE

2.0 Introduction

This section will provide some of the details of the analytical approach employed in the solution of the problem addressed herein. The procedure basically involves the determination of integral representations of the field components, asymptotic evaluation of those integral representations for parameter assignments consistent with far-field conditions, and the subsequent evaluation of the proper power flux expressions in order to set up the Poynting integral.

2.1 *Integral Representations of the Field Components*

We represent the current density of the conducting ring by

$$\bar{J} = Ie^{-in\varphi}\delta(r-r_0)\,\delta(z-\tau)\hat{\varphi} \tag{2.1-1}$$

where $n = \gamma k_0 R$ is an integer, $n \geq 1$, and γ^2 is the effective dielectric constant of the substrate medium. As mentioned earlier, this form for the current density is a good approximation to the current density of anannular-ring structure when the electrical width of the annular-ring is sufficiently small. The Cartesian components of the electric and magnetic field intensities associated with the current density of (2.1-1) are postulated to be of the form.

$$E_z(r,\varphi,z) = E_z(r,z)e^{-in\varphi} \tag{2.1-2}$$

$$H_z(r,\varphi,z) = H_z(r,z)e^{-in\varphi} \tag{2.1-3}$$

Consistent with the circular cylindrical geometry of the problem, the fact that E_z and H_z satisfy the Helmholtz equation, and the absence of physical boundaries along any radial form the z-axis (parallel to the ground plane), one may employ Hankel integral transform representations for both $E_z(r,z)$ and $H_z(r,z)$ of the forms [3,4]

$$E_z(r,z) = \int_0^\infty \tilde{E}_z(\alpha) e^{-k_0(\alpha^2-1)^{1/2}(z-\tau)} J_n(k_0\alpha r)\alpha d\alpha \qquad (2.1\text{-}4)$$

$$H_z(r,z) = \int_0^\infty \tilde{H}_z(\alpha) e^{-k_0(\alpha^2-1)^{1/2}(z-\tau)} J_n(k_0\alpha r)\alpha d\alpha \qquad (2.1\text{-}5)$$

for $z \geq \tau$, where $\tilde{E}_z(\alpha)$ and $\tilde{H}_z(\alpha)$ are ultimately determined via the application of source and continuity conditions at $z = \tau$. From (2.1-4) and (2.1-5) we see that $\tilde{E}_z(\alpha)$ and $\tilde{H}_z(\alpha)$ are the Hankel transforms of $E_z(\tau,\tau)$, and $H_z(\tau,\tau)$, respectively.

It is well known that Maxwell's equations can be arranged so as to express the transverse (to the z-direction) components of the electromagnetic field in terms of the cartesian components E_z and H_z. When this is done and equations (2.1-4) and (2.1-5) are used to express $E_z(r,z)$ and $H_z(r,z)$, one finds the following integral representations for each of the transverse field components [5]:

$$E_\varphi(r,z) = i\left[\frac{n}{k_0 r}\right]\int_0^\infty \tilde{E}_z(\alpha, z)\, J_n(k_0\alpha r)(\alpha^2-1)^{1/2}\frac{d\alpha}{\alpha}$$

$$+ i\zeta_0 \int_0^\infty \tilde{H}_z(\alpha,z)\, J_n'(k_0\alpha r)\, d\alpha \qquad (2.1\text{-}6)$$

$$E_r(r,z) = -\zeta_0\left[\frac{n}{k_0 r}\right]\int_0^\infty \tilde{H}_z(\alpha,z)\, J_n(k_0\alpha r)\frac{d\alpha}{\alpha}$$

$$-\int_0^\infty \tilde{E}_z(\alpha,z)\, J_n'(k_0\alpha r)\,(\alpha^2-1)^{1/2} d\alpha \qquad (2.1\text{-}7)$$

$$H_\varphi(r,z) = i\left[\frac{n}{k_0 r}\right]\int_0^\infty \tilde{H}_z(\alpha,z)\, J_n(k_0\alpha r)(\alpha^2-1)^{1/2}\frac{d\alpha}{\alpha}$$

$$-\frac{i}{\zeta_0}\int_0^\infty \tilde{E}_z(\alpha,z)\, J_n'(\alpha k_0 r) d\alpha \qquad (2.1\text{-}8)$$

$$H_r(r,z) = \frac{1}{\zeta_0}\left[\frac{n}{k_0 r}\right]\int_0^{\infty} \tilde{E}_z(\alpha,z) J_n(k_0\alpha r)\frac{d\alpha}{\alpha}$$

$$-\int_0^{\infty} \tilde{H}_z(\alpha,z) J_n'(k_0\alpha r)(\alpha^2-1)^{1/2} d\alpha \qquad (2.1\text{-}9)$$

where

$$\tilde{E}_z(\alpha,z) = \tilde{E}_z(\alpha) e^{-k_0(\alpha^2-1)^{1/2}(z-\tau)}$$

$$\tilde{H}_z(\alpha,z) = \tilde{H}_z(\alpha) e^{-k_0(\alpha^2-1)^{1/2}(z-\tau)}$$

k_0 is the free space wave number, ζ_0 is the intrinsic impedance of free space, and

$$J_n'(k_0\alpha r) = \left[\frac{d}{dx} J_n(x)\right]\Big|_{x=k_0\alpha r}.$$

Having the field component integral representations of equations (2.1-4) through (2.1-9), one may solve the inhomogeneous boundary valve problem posed by the configuration of Figure 1.1-1 by applying well known source and continuity conditions at $z = \tau$. This procedure yields [Appendix]:

$$\tilde{E}_z(\alpha) = -\frac{(nk_0\zeta_0 I)(n_2^2-\alpha^2)^{1/2}\tan[T(n_2^2-\alpha^2)^{1/2}] J_n(k_0\alpha r_0)}{in_2^2(1-\alpha^2)^{1/2} - (n_2^2-\alpha^2)^{1/2}\tan[T(n_2^2-\alpha^2)^{1/2}]} \qquad (2.1\text{-}10)$$

$$\tilde{H}_z(\alpha) = -\frac{(k_0^2 r_0 I)\alpha J_n'(k_0\alpha r_0)}{i(1-\alpha^2)^{1/2} + (n_2^2-\alpha^2)^{1/2}\cot[T(n_2^2-\alpha^2)^{1/2}]} \qquad (2.1\text{-}11)$$

where $T = k_0\tau$ is the electrical thickness of the substrate.

2.2 *Asymptotic Evaluation of the Field Components*

We will consider in detail the development of the asymptotic form of $E_z(r,z)$ for $k_0(r^2+z^2)^{1/2} = k_0 R \to \infty$. The asymptotic form for each remaining field components follows from the application of the same basic analytical

approach that is illustrated here for $E_z(r,z)$. As one would expect from consideration of equations (2.1-6) through (2.1-9), the leading term of the asymptotic representation for each of the transverse field components is associated with those integrals not preceded by the factor $(k_0 r)^{-1}$.

For analytical convenience we change to a spherical coordinate representation of the variables in the integrand, thus (2.1-4) becomes

$$E_z(R,\vartheta) = \int_0^{\infty} \tilde{E}_z(\alpha) e^{-k_0(\alpha^2-1)^{1/2}(R\cos\vartheta - \tau)} J_n(k_0 \alpha R \sin\vartheta)\alpha d\alpha \qquad (2.2\text{-}1)$$

where $0 < \vartheta < \cos^{-1}\left[\frac{\tau}{R}\right]$. Consideration of the factor $(\alpha^2-1)^{1/2}$ in the exponential term suggests splitting the range of integration so that (2.2-1) becomes

$$E_z(R,\vartheta) = \int_0^1 \tilde{E}_z(\alpha) e^{-ik_0(1-\alpha^2)^{1/2}(R\cos\vartheta - \tau)} J_n(k_0\alpha\, R\, \sin\vartheta)\, \alpha d\alpha$$

$$+ \int_1^{\infty} \tilde{E}_z(\alpha) e^{-k_0(\alpha^2-1)^{1/2}(R\cos\vartheta - \tau)} J_n(k_0\alpha\, R\, \sin\vartheta)\, \alpha d\alpha, \qquad (2,2\text{-}2)$$

where we have used a branch of $(\alpha^2-1)^{1/2}$ where $(\alpha^2-1)^{1/2} = i(1-\alpha^2)^{1/2}$.

The function $\tilde{E}_z(\alpha)$ possesses simple poles $\{\alpha_k\}$ distributed between 1 and n_2 , so the second integral in (2.2-2) yields a sum of residues (associated in this case with TM surface waves) and a Cauchy principal valve integral. Careful evaluation of the principal value integral shows that its leading asymptotic behavior is $O[(k_0R)^{-2}]$, so we have for $(k_0R)\to\infty$,

$$I_2 = \int_1^{\infty} \tilde{E}_z(\alpha) e^{-k_0(\alpha^2-1)^{1/2}(R\cos\vartheta - \tau)} J_n(k_0\alpha\, R\, \sin\vartheta)\alpha d\alpha$$

$$= O[(k_0R)^{-2}] \qquad (2.2\text{-}3)$$

since the surface wave terms have an exponentially decreasing dependence

upon k_0R.

Returning to the first integral in (2.2-2), we employ the well known integral representation

$$J_n(k_0\alpha R\sin\vartheta)=\frac{1}{2\pi}\int_0^{2\pi}e^{i(n\xi-k_0R\alpha\sin\vartheta\sin\xi)}d\xi$$

to yield

$$\begin{aligned}I_1&=\int_0^1\tilde{E}_z(\alpha)e^{-ik_0(1-\alpha^2)^{1/2}(R\cos\vartheta-\tau)}J_n(k_0\alpha R\sin\vartheta)\alpha d\alpha\\&=\frac{1}{2\pi}\int_0^{2\pi}e^{in\xi}\left\{\int_0^1 e^{-ik_0R\psi(\alpha)}\tilde{E}_z(\alpha)e^{iT(1-\alpha^2)^{1/2}}\alpha d\alpha\right\}d\xi\end{aligned}\qquad(2.2\text{-}4)$$

where $T=k_0\tau$ is the electrical thickness of the substrate and

$$\psi(\alpha)=(\sin\vartheta\sin\xi)\alpha+\cos\vartheta(1-\alpha^2)^{1/2}\qquad(2.2\text{-}5)$$

Differentiating $\psi(\alpha)$ yields the result that for $\sin\xi\geq 0$, $\psi(\alpha)$ has a first order stationary point at $0\leq\alpha_0<1$, where

$$\alpha_0=(\sin\vartheta\sin\xi)/(1-\sin^2\vartheta\cos^2\xi)^{1/2}\qquad(2.2\text{-}6)$$

A second differentiation of $\psi(\alpha)$ gives

$$\psi''(\alpha_0)=(1-\sin^2\vartheta\cos^2\xi)^{3/2}/\cos^2\vartheta$$

The result that $\psi(\alpha)$ has a stationary point only for $\sin\xi\geq 0$ suggests rewriting I_1 in (2.2-4) as

$$\begin{aligned}I_1&=\frac{1}{2\pi}\int_0^{\pi}e^{in\xi}\left\{\int_0^1 e^{-ik_0R\psi(\alpha)}\tilde{E}_z(\alpha)e^{iT(1-\alpha^2)^{1/2}}\alpha d\alpha\right\}d\xi\\&+\frac{1}{2\pi}\int_{\pi}^{2\pi}e^{in\xi}\left\{\int_0^1 e^{-ik_0R\psi(\alpha)}\tilde{E}_z(\alpha)e^{iT(1-\alpha^2)^{1/2}}\alpha d\alpha\right\}d\xi\end{aligned}\qquad(2.2\text{-}7)$$

Consideration of the fact that $\alpha\tilde{E}_z(\alpha)$ has a zero of order at least one for $\alpha = 0$ shows that the integral from 0 to 1 in the second term of (2.2-7) can be integrated by parts. When this is done, the boundary terms vanish and a subsequent application of the Riemann-Lebesque lemma yields the conclusion

$$\int_{\pi}^{2\pi} e^{in\xi}\left\{\int_0^1 e^{-ik_0R\psi(\alpha)}\tilde{E}_z(\alpha)\, e^{iT(1-\alpha^2)^{1/2}}\alpha\, d\alpha\right\} d\xi = o\left[(k_0R)^{-1}\right] \qquad (2.2\text{-}8)$$

To this point, then, taking account of (2.2-3), (2.2-7) and (2.2-8) we have

$$E_z(R,\vartheta) = \frac{1}{2\pi}\int_0^{\pi} e^{in\xi}\left\{\int_0^1 e^{-ik_0R\psi(\alpha)}\,\tilde{E}_z(\alpha)e^{iT(1-\alpha^2)^{1/2}}\alpha\, d\alpha\right\}d\xi + o\left[(k_0R)^{-1}\right] \qquad (2.2\text{-}9)$$

Since there is a stationary phase point in $[0, 1]$, the integral from 0 to 1 in the first term of (2.2-9) has the asymptotic behavior [6]

$$\int_0^1 e^{-ik_0R\psi(\alpha)}\tilde{E}_z(\alpha)e^{iT(1-\alpha^2)^{1/2}}\alpha\, d\alpha \sim \frac{1}{(k_0r)^{1/2}} f(\xi)\, e^{-ik_0R(1-\sin^2\vartheta\cos^2\xi)^{1/2}} \qquad (2.2\text{-}10)$$

where

$$f(\xi) = (2\pi)^{1/2}e^{i\frac{\pi}{4}}\, e^{iT[\cos\vartheta/(1-\sin^2\vartheta\cos^2\xi)^{1/2}]} \frac{(\cos\vartheta\sin\vartheta\sin\xi)}{(1-\sin^2\vartheta\cos^2\xi)^{5/4}}\tilde{E}_z\left[\frac{\sin\vartheta\sin\xi}{(1-\sin^2\vartheta\cos^2\xi)^{1/2}}\right] \qquad (2.2\text{-}11)$$

Thus, (2.2-9) may be written as

$$E_z(R,\vartheta) \sim \frac{1}{(k_0R)^{1/2}}\int_0^{\pi} f(\xi)\, e^{in\xi}\, e^{-ik_0R(1-\sin^2\vartheta\cos^2\xi)^{1/2}} d\xi + o\left[(k_0R)^{-1}\right] \qquad (2.2\text{-}12)$$

Considering the phase term $k_0R(1-\sin^2\vartheta\cos^2\xi)^{1/2}$, one sees that it has rapid variation when $k_0R\sin^2\vartheta \gg 1$ and has first order stationary points for $\xi = 0, \frac{\pi}{2}, \pi$. The leading term of the asymptotic representation of the integral in (2.2-12) is therefore associated with $\xi = \frac{\pi}{2}$, since $f(\frac{\pi}{2}) \neq 0$, while $f(0) = f(\pi) = 0$. Hence,

$$\int_0^{\pi} f(\xi)\, e^{i\nu\xi}\, e^{-ik_0R(1-\sin^2\vartheta\cos^2\xi)^{1/2}} d\xi \sim$$

$$(2\pi)^{1/2}\frac{1}{(k_0R)^{1/2}}\frac{f(\frac{\pi}{2})}{\sin\vartheta}e^{-i(k_0R-\frac{\nu\pi}{2}-\frac{\pi}{4})} \qquad (2.2\text{-}13)$$

Finally, use of (2.2-13) with (2.2-11) and (2.2-12) gives

$$E_z(R,\vartheta) \sim (k_0r_0\zeta_0 I)\left[\frac{e^{-ik_0R}}{R}\right] e^{i[(n+1)\frac{\pi}{2}+T\cos\vartheta+\theta_t]}$$

$$\left\{\frac{-\gamma\cos\vartheta\, J_n(k_0r_0\sin\vartheta)\Phi\, tan(T\Phi)}{(n_2^4\cos^2\vartheta+\Phi^2\tan^2(T\Phi))^{1/2}}\right\} \qquad (2.2\text{-}14)$$

where

$$\theta_t = \tan^{-1}\left[\frac{n_2^2\cos\vartheta}{\Phi tan(T\Phi)}\right] \qquad (2.2\text{-}15)$$

and

$$\Phi = (n_2^2 - \sin^2\vartheta)^{1/2} \qquad (2.2\text{-}16)$$

Following a procedure just like the one outlined above for the derivation of the leading asymptotic forms of the remaining field components, one finds

$$E_\phi(R,\vartheta) \sim (k_0 r_0 \zeta_0 I)\left\{\frac{e^{-ik_0R}}{R}\right\} e^{i[(n+1)\frac{\pi}{2} + T\cos\vartheta + \theta_e]}$$

$$\left\{\frac{\cos\vartheta\, J_n'(k_0 r_0 \sin\vartheta)}{(\cos^2\vartheta + \Phi^2 cot^2(T\Phi))^{1/2}}\right\} \qquad (2.2\text{-}17)$$

$$E_r(R,\vartheta) \sim (k_0 r_0 \zeta_0 I)\left\{\frac{e^{-ik_0R}}{R}\right\} e^{i[(n+1)\frac{\pi}{2} + T\cos\vartheta + \theta_t]}$$

$$\left\{\frac{\gamma\cos\vartheta\, cot\ \vartheta\, J_n(k_0 r_0 \sin\vartheta)\Phi tan(T\Phi)}{(n_2^4\cos^2\vartheta + \Phi^2\tan^2(T\Phi))^{1/2}}\right\} \qquad (2.2\text{-}18)$$

$$H_z(R,\vartheta) \sim (k_0 r_0 I)\left\{\frac{e^{-ik_0R}}{R}\right\} e^{i[(n+1)\frac{\pi}{2} + T\cos\vartheta + \theta_c]}$$

$$\left\{\frac{\sin\vartheta\cos\vartheta\, J_n'(k_0 r_0 \sin\vartheta)}{(\cos^2\vartheta + \Phi^2 cot^2(T\Phi))^{1/2}}\right\} \qquad (2.2\text{-}19)$$

$$H_\phi(R,\vartheta) \sim (k_0 r_0 I)\left\{\frac{e^{-ik_0R}}{R}\right\} e^{i[(n+1)\frac{\pi}{2} + T\cos\vartheta + \theta_t]}$$

$$\left\{\frac{\gamma\, cot\ \vartheta J_n(k_0 r_0 \sin\vartheta)\ \Phi\ tan(T\Phi)}{(n_2^4\cos^2\vartheta + \Phi^2\tan^2(T\Phi))^{1/2}}\right\} \qquad (2.2\text{-}20)$$

$$H_r(R,\vartheta) \sim (k_0 r_0 I)\left\{\frac{e^{-ik_0R}}{R}\right\} e^{i[(n+1)\frac{\pi}{2} + T\cos\vartheta + \theta_c]}$$

$$\left\{\frac{-\cos^2\vartheta\, J_n'(k_0 r_0 \sin\vartheta)}{(\cos^2\vartheta + \Phi^2 cot^2(T\Phi))^{1/2}}\right\} \qquad (2.2\text{-}21)$$

where

$$\theta_e = \tan^{-1}\left\{\frac{-\cos\vartheta}{\Phi\ cot(T\Phi)}\right\} \qquad (2.2\text{-}22)$$

In their paper [5], Itoh and Araki do not specifically address the conducting ring or annulus over a grounded substrate, but discuss instead the case of a conducting circular disk over a grounded substrate. We have already referenced Itoh and Araki in Section 2.1 of this report because they too employ Hankel transform integral representations for the solution of the Helmholtz equation

above and below the source plane.

In equation (17) of their paper, Itoh and Araki give an expression for the field associated Hankel transforms $\tilde{E}_{(+)}(\alpha)$ and $\tilde{E}_{(-)}(\alpha)$ in terms of the current associated Hankel transforms $\tilde{J}_{(+)}(\alpha)$ and $\tilde{J}_{(-)}(\alpha)$. This expression results from the solution of the inhomogeneous boundary value problem for the disk. Once the current associated transforms have been determined, the field associated transforms are determined and the problem is formally solved. Indeed, employing the field equivalence principle and a saddle point asymptotic analysis, Itoh and Araki derive their equations (30) and (31), which express the far-zone electric field components E_ϑ and E_φ directly in terms of the field associated transforms $\tilde{E}_{+}(\alpha)$ and $\tilde{E}_{(-)}(\alpha)$. The paper proceeds to discuss the use of Galerkin's method as a means of determining the current associated transforms for the disk.

If, however, one assumes that the current on the disk is identically zero except for a current about its periphery of the form given in equation (2.1-1), then one can determine the current associated transforms to be

$$\tilde{J}_{(+)}(\alpha) = iI r_0 J_{n+1}(\alpha k_0 r_0) \tag{2.2-23}$$

$$\tilde{J}_{(-)}(\alpha) = -iI\gamma_0 J_{n-1}(\alpha k_0 r_0) \tag{2.2-24}$$

Using (2.2-23) and (2.2-24) to determine the field associated transforms, and use of the field associated transforms in equations (30) and (31) of Itoh and Araki yields $|E_\vartheta(R,\vartheta)|$ as derived from (2.2-14) and (2.2-18) and $|E_\varphi(R,\vartheta)|$ as derived from (2.2-17). To this extent, then, the analysis of Itoh and Araki is in agreement with that presented within this report. It is worthy of note that the use by Itoh and Araki of the field equivalence principle in conjunction with a saddle point method to generate far-field expressions differs discernibly from the

direct, successive stationary phase evaluations of the integral representations of the fields employed to generate the far-field expressions appearing in this report.

2.3 *The Skywave Power Integral*

To evaluate the time average power flow due to skywave radiation from the ring, we use $E_\phi = E_r\cos\vartheta - E_z\sin\vartheta$ and $H_\vartheta = H_r\cos\vartheta - H_z\sin\vartheta$ along with the asymptotic forms of the field components (derived in the previous sub- section) in the Poynting integral

$$\mathbf{P} = \pi R_a \int_0^{\frac{\pi}{2}} (E_\phi H_\varphi^* - E_\varphi H_\vartheta^*) R^2 \sin\vartheta \, d\vartheta.$$

The resultant form of the time average power flow through a hemisphere of radius R above the substrate (as $r \to \infty$) is given by

$$\mathbf{P} = [\pi(k_0 r_0)^2 \zeta_0 I^2] \left\{ \gamma^2 \int_0^{\frac{\pi}{2}} \frac{\cos^2\vartheta \, J_n^2(k_0 r_0 \sin\vartheta) \Phi^2 \tan^2(T\Phi) \, d\vartheta}{\sin\vartheta (n_2^4 \cos^2\vartheta + \Phi^2 \tan^2(T\Phi))} \right.$$

$$\left. + \frac{1}{4} \int_0^{\frac{\pi}{2}} \frac{\cos^2\vartheta \sin\vartheta [J_{n-1}(k_0 r_0 \sin\vartheta) - J_{n+1}(k_0 r_0 \sin\vartheta)]^2 d\vartheta}{\cos^2\vartheta + \Phi^2 cot^2(T\Phi)} \right\}. \qquad (2.3\text{-}1)$$

where Φ is given in equation (2.2-16).

Equation (2.3-1) involves finite integrals with closed form integrands, hence the integrals can be readily evaluated by numerical methods. One must note, however, that since $n = \gamma k_0 r_0$, practical use of (2.3-1) requires either that one know the resonant frequency (hence k_0) for a physical configuration of interest [7] or that one know γ for that configuration. For application of (2.3-1) in this report we shall consider physical configurations for which $k_0 r_0$ is large enough and k_0 is small enough to allow use of the (narrow) straight strip, quasistatic

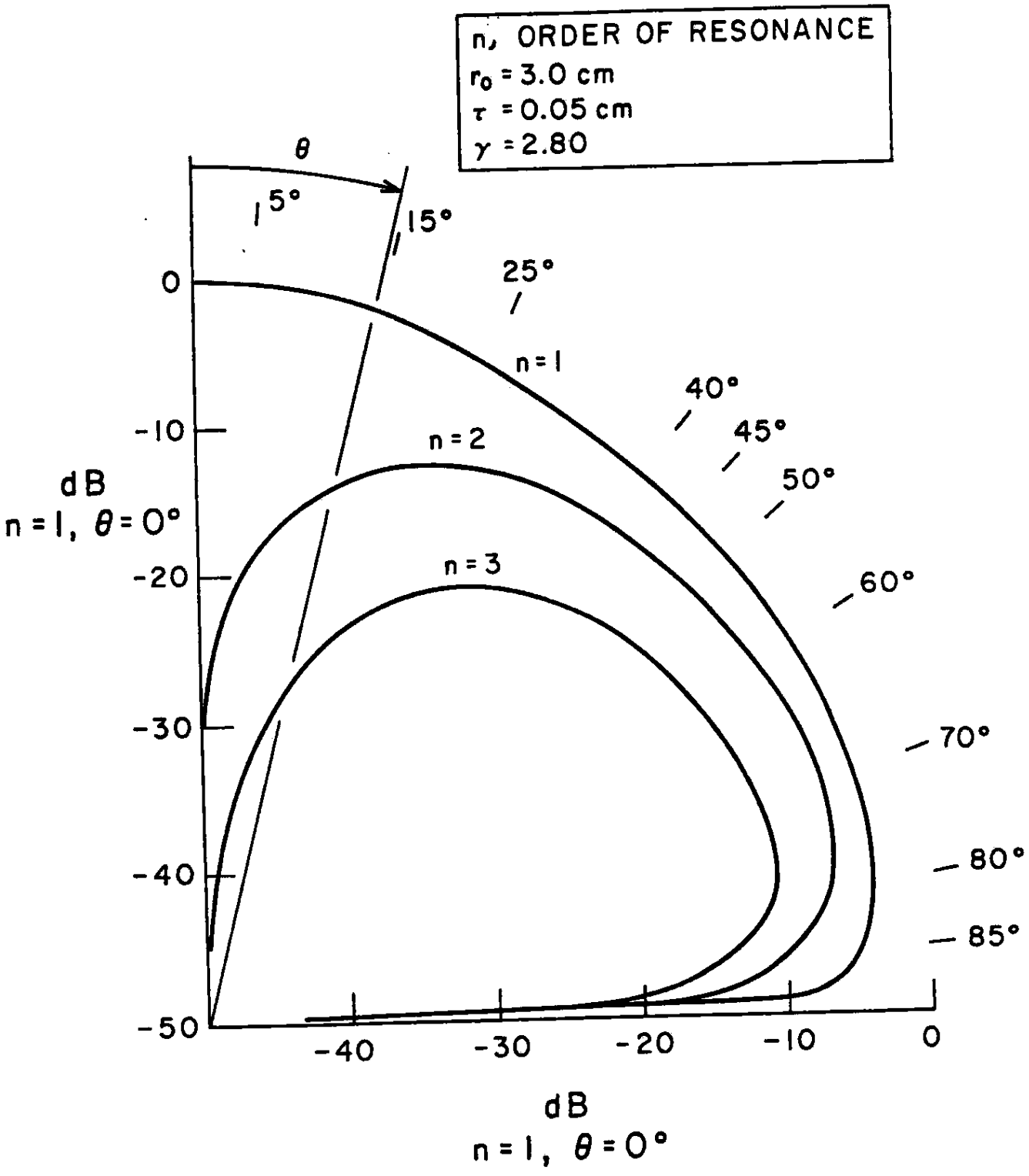

Fig. 2.3-1. Polar Plot of Power Patterns for the First Three Resonant Modes

approximation to $\gamma^{\prime\prime}$ given by Kuester [8] .

Figure 2.3-1 is a power pattern plot derived from the power density expression used to obtain P in equation (2.3-1), the power patterns for the first three resonant modes are shown for typical integrated microwave physical parameter values and are plotted in decibels relative to the value of the power pattern for the first resonant mode at $\vartheta = 0°$. Notice that only for the first resonant mode of the ring current is there radiation in the broadside ($\vartheta = 0°$) direction, and indeed, that the power pattern for the first order of resonance has a global maximum for $\vartheta = 0°$. The higher resonant modes exhibit an increasingly endfire character (the majority of the power radiates at angles ϑ approaching 90°) and smaller absolute amounts of radiated power for all values of ϑ relative to the first resonant mode.

Section 3. COMPARISON WITH PREVIOUS RESULTS

3.0 Introduction

Within this section we will briefly compare the results presented within this report to those obtained in two previous papers, both of which directly address the problem of skywave radiation from electrically narrow annular rings over a grounded substrate. When reading this section one should recall the favorable comparison with Stoh and Araki described in Section 2.2 of this report.

3.1 Results of van der Pauw

In his paper [1] van der Pauw discusses a method for determining the radiation loss from a variety of microstrip configurations when the width of the conducting strip and the thickness of the dielectric substrate are small compared to wavelength. Of interest here is van der Pauw's expression W_1 given in his equation (34) for the skywave (space wave) radiated power from a "circular resonator." Restoring dimensions to W_1 , making the identifications $\gamma = (LC)^{1/2}/(\mu_0\varepsilon_0)^{1/2}$, and $z = \cos\vartheta$ and after some algebraic rearrangement, one has (for a unit current magnitude)

$$P_{VDP} = (\zeta_0 \pi T^2)\left\{\left[\frac{1}{n_2^4}\right]\int_0^{\frac{\pi}{2}} J_1^2\left[\frac{\sin\vartheta}{\gamma}\right]\frac{(n_2^2 - \sin^2\vartheta)^2}{\sin\vartheta}d\vartheta\right.$$

$$+\left[\frac{1}{4\gamma^2}\right]\int_0^{\frac{\pi}{2}}\cos^2\vartheta\sin\vartheta\left[J_0\left[\frac{\sin\vartheta}{\gamma}\right] - J_2\left[\frac{\sin\vartheta}{\gamma}\right]\right]^2 d\vartheta$$

$$\left.-\int_0^{\frac{\pi}{2}}\frac{\cos^2\vartheta}{\sin\vartheta}J_1^2\left[\frac{\sin\vartheta}{\gamma}\right]d\vartheta\right\}. \qquad (3.1\text{-}1)$$

To compare P_{VDP} with P as given in (2.3-1), the power patterns associated with these power integrals are plotted in Figure 3.1-1. The power patterns are

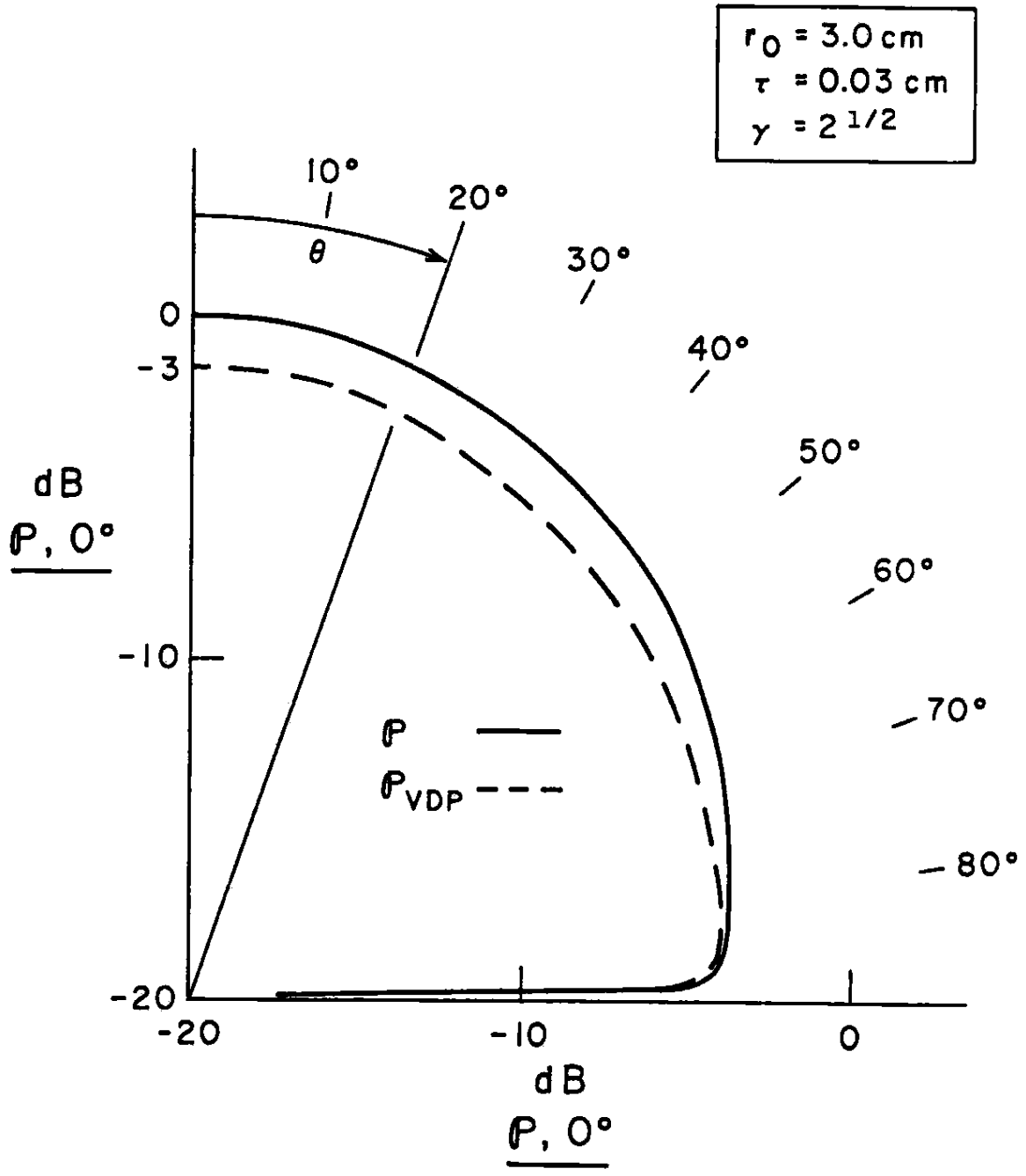

Fig. 3.1-1. Power Patterns Associated With $\mathcal{P}(n=1)$ and $\mathcal{P}_{VDP}$

plotted in a polar fashion with amplitudes given in decibels relative to the power pattern associated with **P** for $\vartheta = 0°$. Notice that these plots are for the first order of resonance only, since van der Pauw's W_1 [hence P_{VDP} in (3.1-1)] was derived assuming a current form consistent with the first order of resonance.

The discrepancy illustrated in these plots can be made clear analytically by considering (2.3-1) for $T \ll 1$. Multiplying the numerator and denominator by n_2^4 and then adding and subtracting $[J_n^2(k_0 r_0 \sin\vartheta)\Phi^4 \tan^4(T\Phi)]$ in the numerator of the first integral, then use of the small argument forms for $\tan(T\Phi)$ and $cot\,(T\Phi)$ in both integrals yields (for unit current magnitude)

$$\mathbf{P} = (\zeta_0 \pi T^2)\left\{\left[\frac{1}{n_2^4}\right]\int_0^{\frac{\pi}{2}} J_1^2\left[\frac{\sin\vartheta}{\gamma}\right]\frac{(n_2^2 - \sin\vartheta)^2}{\sin\vartheta}d\vartheta\right.$$

$$\left. + \left[\frac{1}{4\gamma^2}\right]\int_0^{\frac{\pi}{2}} \cos^2\vartheta \sin\vartheta\left[J_0\left[\frac{\sin\vartheta}{\gamma}\right] - J_2\left[\frac{\sin\vartheta}{\gamma}\right]\right]^2 d\vartheta\right\}$$

$$+ O(T^4). \qquad (3.1\text{-}2)$$

where $T \ll 1$. Comparing (3.1-2) with (3.1-1) shows that to leading order in T ,

$$\mathbf{P} - \mathbf{P}_{VDP} = (\zeta_0 \pi T^2)\int_0^{\frac{\pi}{2}} \frac{\cos^2\vartheta}{\sin\vartheta} J_1^2\left[\frac{\sin\vartheta}{\gamma}\right]d\vartheta \qquad (3.1\text{-}3)$$

The difference in (3.1-3) is not insignificant, hence our comparison with van der Pauw, while close in some respects, does not reveal sufficient agreement between the results to justify the conclusion that either approach has been independently verified.

3.2 Results of Wood

In his paper [2], Wood addresses the problem of an electrically narrow annular ring over an electrically thin grounded substrate by applying the

equivalence principle and the low-frequency equivalent width of the ring to specify the magnitude and location of equivalent magnetic currents. These magnetic currents account for the electric field fringing at the edges of the ring and constitute the effective radiation sources.

For the skywave radiated power from such a ring, Wood obtains [Wood's equation (7)]

$$P_r = \frac{2k_0r_0(W =)^2V^2\pi}{\lambda^2\eta} F_\beta(k_0r_0) \qquad (3.2\text{-}1)$$

where $W = = \frac{\eta_0 T}{Z_m \gamma}$, Z_m is the microstrip line impedance, V is the microstrip line voltage, λ is the free-space wavelength, $\beta = \gamma k_0 r_0$, and $F_\beta(k_0r_0)$ is a complicated double-infinite series which is illustrated graphically for various values $\gamma^2 = \varepsilon_{eff}$ in Wood's Figure 3.

In order to compare Wood's P_r with P in (2.3-1), we use $I^2 = V^2/Z_m^2$ in (3.2-1) so that rearrangement gives

$$\mathbf{P}_{Wood} = [\pi(k_0r_0)^2\zeta_0 I^2]\left[\frac{T^2}{2\pi^2\gamma}\right] F_\beta(k_0r_0). \qquad (3.2\text{-}2)$$

Manipulation of (2.3-1) as was done to obtain (3.1-2) and neglecting terms of order T^4 gives

$$\mathbf{P} = [\pi(k_0r_0)^2\zeta_0 I^2]\left[\frac{T^2}{2\pi^2\gamma}\right] \Gamma(k_0r_0,\gamma) \qquad (3.2\text{-}3)$$

where

$$\Gamma(k_0 r_0,\gamma) = 2\pi^2\left\{\gamma^3 \int_0^{\frac{\pi}{2}} \frac{J_n^2(k_0 r_0 \sin\vartheta)\left[1 - \left[\frac{\sin\vartheta}{n_2}\right]^2\right]^{\frac{1}{2}} d\vartheta}{\sin\vartheta}\right.$$

$$\left. + \frac{\gamma}{4}\int_0^{\frac{\pi}{2}} \cos^2\vartheta \sin^2\vartheta [J_{n-1}(k_0 r_0 \sin\vartheta) - J_{n+1}(k_0 r_0 \sin\vartheta)]^2 d\vartheta\right\}. \qquad (3.2\text{-}4)$$

Comparison of (3.2-3) with (3.2-2) suggests that P_{Wood} and P are in agreement to the extent that $F_\beta(k_0 r_0)$ and $\Gamma(k_0 r_0,\gamma)$ are in agreement. A graphical comparison of $F_\beta(k_0 r_0)$ and $\Gamma(k_0 r_0,\gamma)$ is given in Figure 3.2-1. The values shown for $F_\beta(k_0 r_0)$ are taken directly from Wood's Figure 3, and the continuous as opposed to discrete nature of these plots follows from the fact that Wood considers some microstrip structures for which his β (our n) is not necessarily an integer and has derived $F_\beta(k_0 r_0)$ to be applicable for those cases as well. In our case, since $n=\gamma k_0 r_0$, specification of n and γ determines $k_0 r_0$ so that $\Gamma(k_0 r_0,\gamma)$ assumes only those discrete values associated with ring current resonance.

Consideration of Figure 3.2-1 shows that a significant difference exists between $F_\beta(k_0 r_0)$ and $\Gamma(k_0 r_0,\gamma)$ for $\gamma = 1$, but that the values of these functions tend toward coincidence as γ increases.

Further insight into the mechanism of discrepancy between these results can be gained through consideration of the fact that γ is roughly proportional to n_2, so that the tendency toward coincidence of $F_\beta(k_0 r_0)$ and $\Gamma(k_0 r_0,\gamma)$ can be correlated with an increase in n_2. This suggests considering a variant of $\Gamma(k_0 r_0,\gamma)$ in which the explicit dependence on n_2 is removed in such a way that the resultant expression merges with that for $\Gamma(k_0 r_0,\gamma)$ as n_2 increases. Consideration of the first integral in (3.2-4) suggests the candidate expression

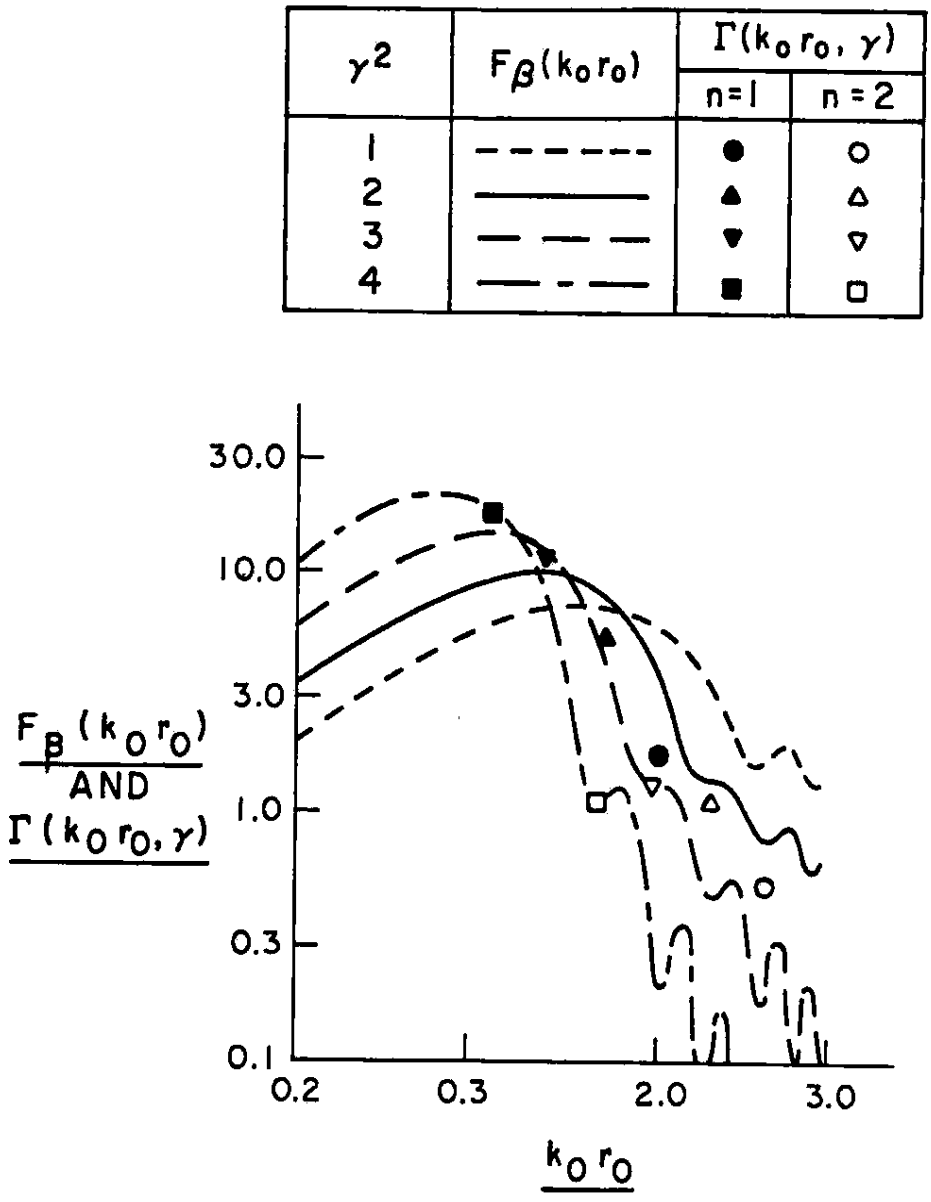

Fig. 3.2-1. A Graphical Comparison of $F_\beta(k_0 r_0)$ and $\Gamma(k_0 r_0, \gamma)$ for the First Two Resonant Modes

$$\Gamma_e(k_0 r_0, \gamma) = 2\pi^2 \left\{ \gamma^3 \int_0^{\frac{\pi}{2}} \frac{J_n^2(k_0 r_0 \sin\vartheta)}{\sin\vartheta} d\vartheta \right.$$

$$\left. + \frac{\gamma}{4} \int_0^{\frac{\pi}{2}} \cos^2\vartheta \sin\vartheta \left[J_{n-1}(k_0 r_0 \sin\vartheta) - J_{n+1}(k_0 r_0 \sin\vartheta) \right]^2 d\vartheta \right\} \qquad (3.2\text{-}5)$$

as a function more consistent with $F_\beta(k_0 r_0)$. That this is indeed the case is verified in the graphical comparison of Figure 3.2-2.

We see then, that it is the factor $\left[1 - \left(\frac{\sin\vartheta}{n_2}\right)^2\right]^{1/2}$ in the integrand of the first integral in (3.2-4) that embodies the significant difference between the expressions for **P** and $\mathbf{P}_{wood}$. The fact that the primary discrepancy between **P** and $\mathbf{P}_{wood}$ should involve a term which explicitly contains n_2 is not surprising, since n_2 appears naturally in **P** as a result of the solution of the inhomogeneous boundary value problem for the conducting ring over a grounded substrate. It is precisely the fact that Wood does not resort to an explicit solution of this inhomogeneous boundary value problem that most dramatically characterizes the difference in analytical approach between Wood's formulation of the problem and that presented herein (note that van der Pauw solves the inhomogeneous boundary value problem to obtain the "impedance dyadic" used in his paper).

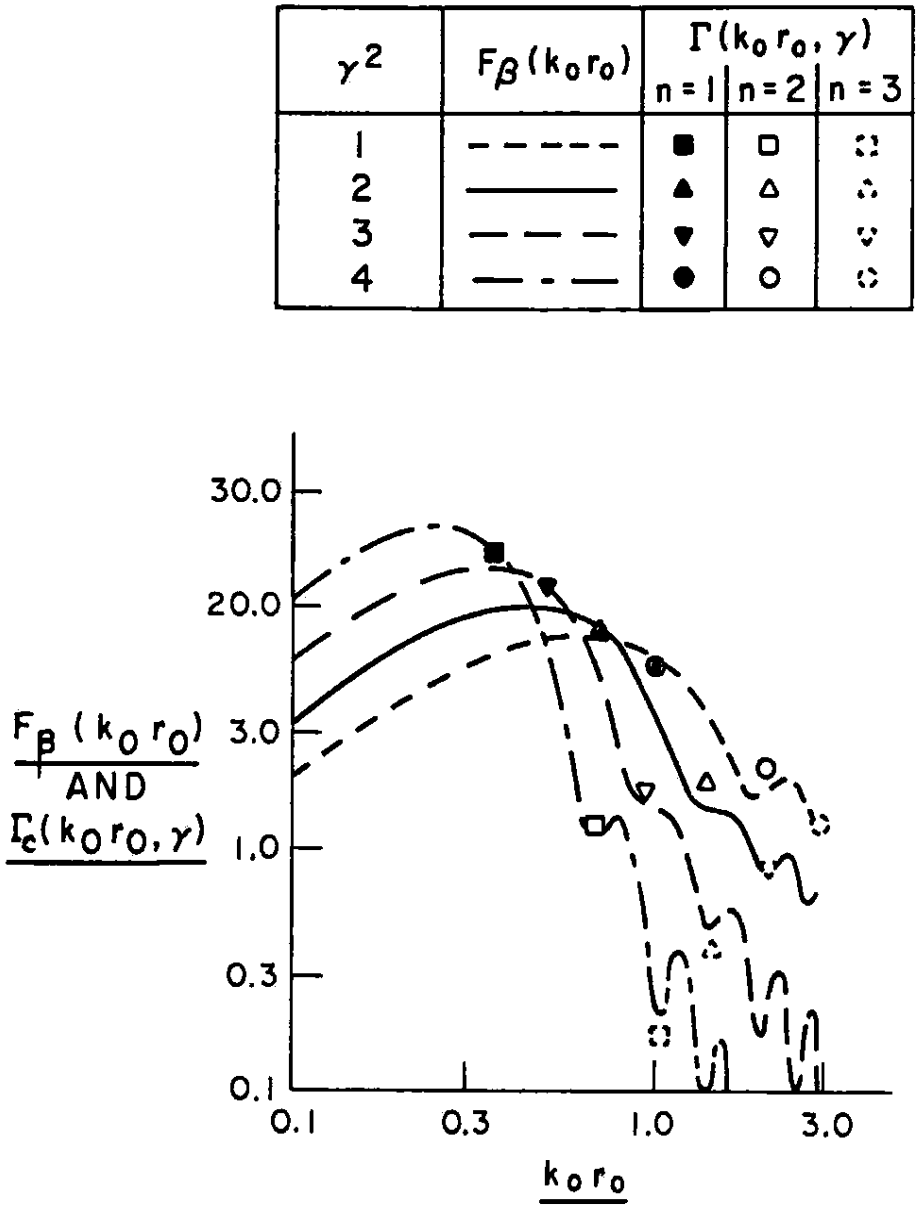

Fig. 3.2-2. A Graphical Comparison of $F_\beta(k_0 r_0)$ and $\Gamma_c(k_0 r_0, \gamma)$ for the First Three Resonant Modes

Section 4

APPROXIMATE REPRESENTATIONS FOR THE SKYWARE RADIATED POWER INTEGRAL

4.0 Introduction

Within this section we will present and summarily discuss a pair of approximate expressions derived from the integral representation of P. In the first case we shall consider the result for $n = 1, N_2 \gg 1$, and $T \ll 1$. In the second instance, we consider the case in which $n \gg 1$ and $T \ll 1$. The resultant expressions for P allow reasonably accurate evaluations of P without the need for numerical integration.

4.1 The First Order of Resonance, Electrically Thin Substrates, $n_2 \gg 1$.

With $n = 1, T \ll 1$, and neglecting terms of order T^4, equation (3.1-2) can be written as

$$P \approx [\pi \zeta_0 I^2 T^2] \left\{ \int_0^{\frac{\pi}{2}} J_1^2 (k_0 r_0 \sin \vartheta) \frac{d\vartheta}{\sin \vartheta} + \left[\frac{1}{\gamma^2}\right] \int_0^{\frac{\pi}{2}} \cos^2 \vartheta \sin \vartheta [J_1'(k_0 r_0 \sin \vartheta)]^2 d\vartheta \right\}. \tag{4.1-1}$$

Using the results [9]

$$\int_0^{\frac{\pi}{2}} J_1^2(\mu \sin x) \frac{dx}{\sin x} = \frac{1}{2\mu}[\mu - J_1(2\mu)]$$

$$\int_0^{\frac{\pi}{2}} \sin x \, J_1^2 (\mu \sin x) dx = \frac{1}{2\mu}\left[\int_0^{2\mu} J_0(x) dx - 2 J_1(2\mu)\right]$$

and

$$\int_0^{\frac{\pi}{2}} \sin\vartheta \cos\vartheta \, J_1^2(\mu \sin\vartheta) d\vartheta = \frac{1}{\mu^2}\left\{-\frac{1}{2} + J_0(\mu) - \frac{1}{2}J_0^2(\mu) - \mu J_1(\mu)\,[J_0(\mu) - 1]\right\},$$

the first integral in (4.1-1) is evaluated directly, and repeated application of integration by parts yields the second integral, whence (letting $\mu = k_0 r_0$)

$$\mathbf{P} \approx [\pi \zeta_0 I^2 T^2]\left\{\frac{2}{3}J_0(\mu) - \frac{1}{2}J_0(2\mu) - \frac{1}{3}(1 + J_0^2(\mu)) + \frac{1}{2}\left[\frac{\mu}{3} + \frac{1}{2\mu}\right]\int_0^{2\mu} J_0(x)dx + \frac{2\mu}{3}J_1(\mu)(1 - J_0(\mu)) - \frac{\mu}{3}J_1(2\mu) - \frac{\mu^3}{3}J_1^2(\mu)\right\} \qquad (4.1\text{-}2)$$

All of the terms in (4.1-2) which involve Bessel functions are tabulated [10]. The expression for **P** given in (4.1-2) has been compared with numerically integrated values of **P** as determined by (4.1-1), and the results so obtained indicate that no more than a 3.0% relative error exists between the values obtained for **P** by these two methods. For the sake of this investigation, the result in equation (4.1-2) has served as a useful check on the accuracy of our numerical integration procedure.

4.2 Large Order of Resonance, Electrically Thin Substrate

We consider **P** as given in (2.3-1) for $T \ll 1$, in which case we have

$$\mathbf{P} = [\pi(k_0 r_0)^2 \zeta_0 I^2](I_1 + I_2) \qquad (4.2\text{-}1)$$

where

$$I_1 \approx \gamma^2 T^2 \int_0^{\frac{\pi}{2}} \frac{\cos^2\vartheta \, J_n^2\left[\frac{n \sin\vartheta}{\gamma}\right](n_2^2 - \sin^2\vartheta)^2 d\vartheta}{\sin\vartheta[n_2^4 \cos^2\vartheta + (n_2^2 - \sin^2\vartheta)^2 T^2]} \qquad (4.2\text{-}2)$$

$$I_2 \approx \int_0^{\frac{\pi}{2}} \frac{\cos^2\vartheta \sin\vartheta \left[J_n'\left(\frac{n \sin\vartheta}{\gamma}\right)\right]^2 d\vartheta}{[\cos^2\vartheta + T^{-2}]} \tag{4.2-3}$$

Considering first I_1 for $n \gg 1$, we employ the Debye expansion [10] of J_n which gives

$$J_n^2\left(\frac{n \sin\vartheta}{\gamma}\right) \sim \frac{e^{-nf(\vartheta)}}{2\pi n\left[1-\frac{\sin^2\vartheta}{\gamma^2}\right]^{\frac{1}{2}}} \tag{4.2-4}$$

where

$$f(\vartheta) = \log\left[\frac{1+\left[1-\frac{\sin^2\vartheta}{\gamma^2}\right]^{\frac{1}{2}}}{1-\left[1-\frac{\sin^2\vartheta}{\gamma^2}\right]^{\frac{1}{2}}}\right] - 2\left[1-\frac{\sin^2\vartheta}{\gamma^2}\right]^{\frac{1}{2}} \tag{4.2-5}$$

Differentiating $f(\vartheta)$ twice gives $f'(\frac{\pi}{2}) = 0$ and $f''(\frac{\pi}{2}) = \frac{2}{\gamma}(\gamma^2-1)^{\frac{1}{2}}$ hence use of (4.2-4) in (4.2-2) yields a Laplace integral [6], the major contribution of which comes from a small neighborhood about $\frac{\pi}{2}$. Thus using $s = \frac{\pi}{2} - \vartheta$ in (4.2-2) after employing the substitution of (4.2-4), we have

$$I_1 \sim \left[\left(1-\frac{1}{n_2^2}\right)^2 T^2\gamma^3 \frac{e^{-f(\frac{\pi}{2})}}{2\pi n(\gamma^2-1)^{\frac{1}{2}}}\right] \int_0^{\infty} \frac{s^2 e^{-n(1-\frac{1}{\gamma^2})^{\frac{1}{2}}s^2} ds}{s^2 + T^2(1-\frac{1}{n_2^2})^2}. \tag{4.2-6}$$

The integral in (4.2-6) is well known [11], whence

$$I_1 \sim \left[\frac{\gamma^3 T^3(1-\frac{1}{n_2^2})^3}{4\pi^{\frac{1}{2}} n(\gamma^2-1)^{\frac{1}{2}}}\right]\left\{\Theta^{-\frac{1}{2}} - \pi^{\frac{1}{2}} e^{\Theta} Erfc\left[\Theta^{\frac{1}{2}}\right]\right\} e^{-nf(\frac{\pi}{2})} \tag{4.27}$$

where

$$\Theta = n(1-\frac{1}{\gamma^2})^{\frac{1}{2}} T^2(1-\frac{1}{n_2^2})^2 \tag{4.2-8}$$

Observing the integrand of (4.2-6) reveals that we must refine our requirement that $n \gg 1$. In order for the asymptotic expansion of I_1 to be valid, we must have $n(1 - \frac{1}{\gamma^2})^{1/2} \gg 1$. However, a careful analysis of the conditions under which the Debye expansion takes the form of (4.2-4) reveals an even more stringent condition,

$$n(1 - \frac{1}{\gamma^2})^{5/2} \gg 1 \tag{4.2-9}$$

Equation (4.2-9) is more stringent in the sense that if (4.2-9) is satisfied, then certainly $n(1 - \frac{1}{\gamma^2})^{1/2} \gg 1$.

Now, considering I_2 in (4.2-3) for n consistent with (4.2-9), we proceed in a way similar to that followed in deriving (4.2-7). A result analogous to (4.2-4) is once again obtained using the Debye expansion for J_n whence

$$\left[J_n'\left[\frac{n}{\gamma}\sin\vartheta\right]\right]^2 = \frac{\gamma^3 \sin^2\vartheta\, C^2(\vartheta) e^{-nf(\vartheta)}}{8\pi n^3(\gamma^2 - \sin^2\vartheta)^{5/2}} \tag{4.2-10}$$

where

$$C^2(\vartheta) = 1 + \frac{2n(\gamma^2 - \sin^2\vartheta)^{3/2}}{\gamma \sin^2\vartheta} \tag{4.2-11}$$

and $f(\vartheta)$ is given in (4.2-5). We therefore have another Laplace integral that assumes the form

$$I_2 \sim \left\{\frac{\gamma[\gamma + 2n(\gamma^2 - 1)^{3/2}]^2\, T^2 e^{-nf(\frac{\pi}{2})}}{8\pi n^3(\gamma^2 - 1)^{5/2}}\right\} \int_0^\infty s^2 e^{-n(1-\frac{1}{\gamma^2})^{1/2}s^2}\, ds \tag{4.2-12}$$

The integral in (4.2-12) is well known [11], whence

$$I_2 \sim \left\{\frac{\gamma[\gamma + 2n(\gamma^2-1)^{3/2}]^2(1-\frac{1}{n^2_2})^3 T^5 e^{-nf(\frac{\pi}{2})}}{32\pi^{1/2} n^3 (\gamma^2 - 1)^{5/2}}\right\} \Theta^{-3/2} \tag{4.2-13}$$

where Θ is given in (4.2-8).

Combining the results from (4.2-7) and (4.2-13) in (4.2-1) gives the result

$$\mathbf{P} \sim \frac{[\pi(k_0 r_0)^2 \zeta_0 f^2][\gamma T(1 - \frac{1}{n_2^2})]^3}{4\pi^{1/2} n\ (\gamma^2 - 1)^{1/2}}$$

$$\left\{\left[\Theta^{-1/2} - \pi^{1/2} e^{\Theta}\ Erfc\left[\Theta^{1/2}\right]\right] + \left\{\frac{[1 + 2(\frac{n}{\gamma})(\gamma^2 - 1)^{3/2}]^2}{8n^2(\gamma^2 - 1)^2}\right\} T^2 \Theta^{-3/2}\right\} e^{-nf(\frac{\pi}{2})} \quad (4.2\text{-}14)$$

Figure 4.2-1 is a graphical comparison of P (normalized to T^2) as computed from (4.2-1), (4.2-2), and (4.2-3) via numerical integration to P (normalized to T^2) as computed by the use of (4.2-14). Violation of the requirement represented in (4.2-9) results in significant errors for γ near to 1, but reasonable agreement is seen for $\gamma^2 \geq 2$, even for $n = 1$, in which case the relative error is less than 30%. The curves for $n = 2$ and 3 in Figure 4.2-1 reveal less than 5% relative error for $\gamma^2 \geq 4$, and relative errors less than 20% for $\gamma^2 = 2$.

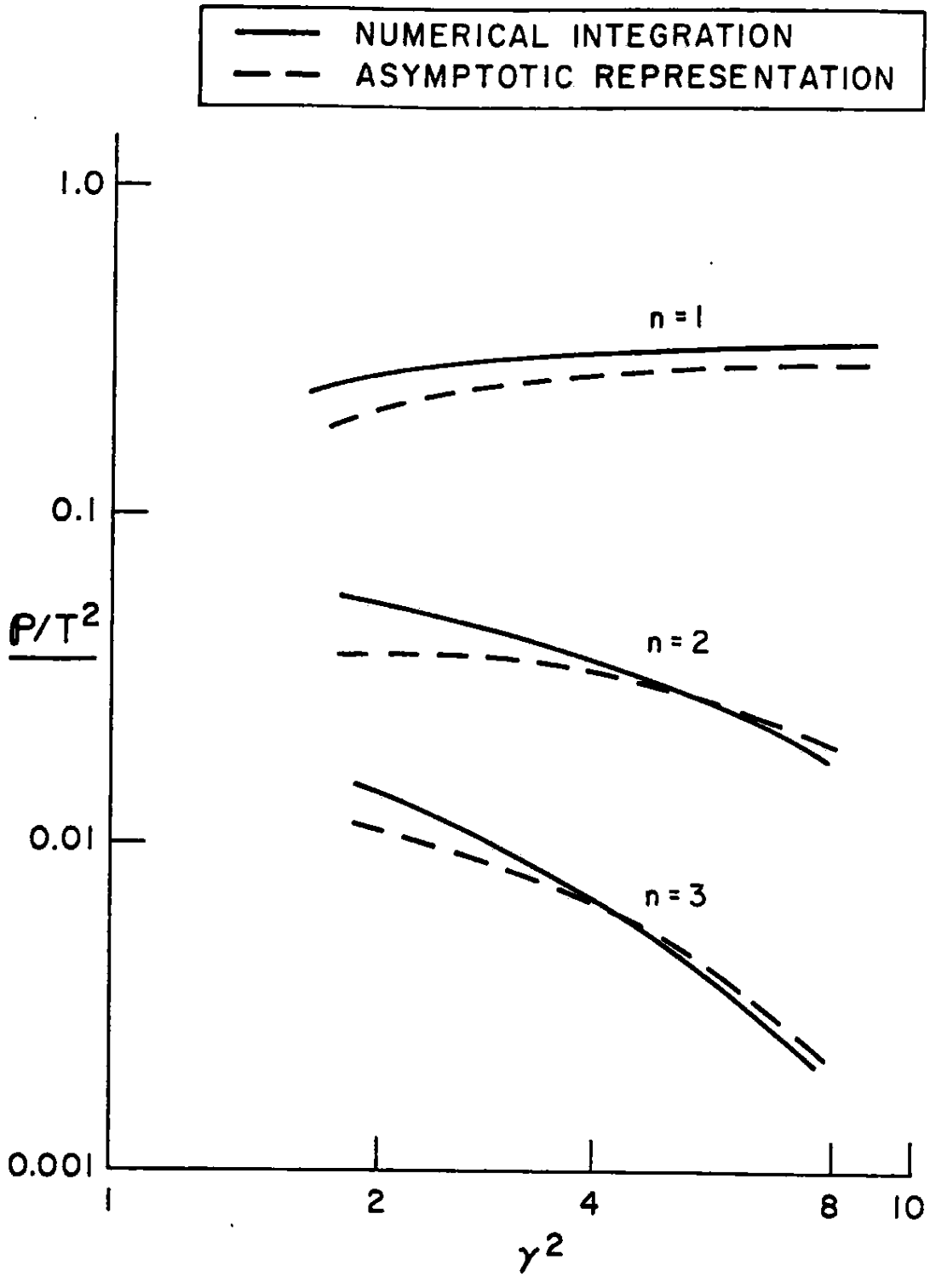

Fig. 4.2-1. A Comparison of Numerically Integrated and Asymptotically Approximated Power Expressions

References

[1] L. J. van der Pauw, " The Radiation of Electromagnetic Power by Microstrip Configurations," *IEEE Trans. Microwave Theory Tech.*, vol. MTT-25, No. 9, pp. 719-725 (1977).

[2] C. Wood, "Curved Microstrip Lines as Compact Wideband Circularly Polarized Antennas," *IEE J. Microwaves, Opt. & Acoust.*, Vol. 3, No. 1, pp. 5-13 (1979).

[3] R. Harrington, *Time-Harmonic Electromagnetic Fields*. New York: McGraw Hill, 1961.

[4] A. Sommerfeld, *Partial Differential Equations in Physics*. New York: Academic Press, 1949.

[5] T. Itoh, K. Araki, "Hankel Transform Domain Analysis of Open Circular Microstrip Radiating Structures," *IEEE Trans. Antennas Propagat.*, Vol. AP-29,No. 1, pp. 84-89 (1981).

[6] N. Bleistein, R. Handelsmann, *Asymptotic Expansions of Integrals*. New York: Holt, Rinehart, Winston, 1975.

[7] R. Pregla, S. Pintzos, "A Simple Method for Computing the Resonant Frequencies of Microstrip Ring Resonators," *IEEE Trans. Microwave Theory Tech.*, Vol.MTT-26, No. 10, pp. 809-813 (1978).

[8] E. Kuester, "Accurate Approximations for a Function Appearing in the Analysis of Microstrip," submitted to *IEEE Trans. Microwave Theory Tech.*

[9] Y. Luke, *Integrals of Bessel Functions*. New York: McGraw-Hill, 1962.

[10] M. Abramowitz, I. Stegun, *Handbook of Mathematical Functions*. U.S. Department of Commerce, National Bureau of Standards Applied Math Series - 55; 10th printing, 1972.

[11] I. Gradshteyn, I Ryzhik, *Table of Integrals, Series, and Products*. New York: Academic Press, 1980.

Appendix

SOLUTION OF THE INHOMOGENEOUS BOUNDARY VALUE PROBLEM FOR THE HANKEL TRANSFORMS $\tilde{E}_z$ AND $\tilde{H}_z$

Representing $E_z(r,z)$ and $H_z(r,z)$ as

$$E_z(r,z) = \int_0^\infty \tilde{E}_z(\alpha,z) J_n(k_0 \alpha r) \alpha d\alpha \tag{A-1}$$

$$H_z(r,z) = \int_0^\infty \tilde{H}_z(\alpha,z) J_n(k_0 \alpha r) \alpha d\alpha \tag{A-2}$$

where $\tilde{E}_z(\alpha,z)$ and $\tilde{H}_z(\alpha,z)$ are Hankel transforms of E_z and H_z respectively, and noting that E_z and H_z satisfy the reduced Helmholtz equation

$$\left\{\frac{1}{r}\frac{\partial}{\partial r} r \frac{\partial}{\partial r} + \frac{\partial^2}{\partial z^2} + k_{1,2}^2 - \frac{n^2}{r^2}\right\} \begin{bmatrix} E_z(r,z) \\ H_z(r,z) \end{bmatrix} = \begin{bmatrix} 0 \\ 0 \end{bmatrix} \tag{A-3}$$

we conclude

$$\left\{\frac{\partial^2}{\partial z^2} + k_0^2 \left(n_{1,2} - \alpha^2\right)\right\} \begin{bmatrix} \tilde{E}_z(\alpha,z) \\ \tilde{H}_z(\alpha,z) \end{bmatrix} = \begin{bmatrix} 0 \\ 0 \end{bmatrix} \tag{A-4}$$

Solving (A-4) for $z \geq \tau$ and then for $0 \leq z \leq \tau$, using the fact that $H_z = E_r = E_\varphi = 0$ at $z = 0$ imply [see equations (2.1-6) and (2.1-7)] that $\tilde{H}_z = \dfrac{\partial \tilde{E}_z}{\partial z} = 0$ at $z = 0$, we find

$$\tilde{E}_z(\alpha,z) = \begin{cases} \tilde{E}_1(\alpha)\, e^{-k_0 \alpha u_1 (z-\tau)}, & z \geq \tau \\ \tilde{E}_2(\alpha) \cosh\left(k_0 u_2 z\right), & z \leq \tau \end{cases} \tag{A-5}$$

$$\tilde{H}_z(\alpha,z) = \begin{cases} \tilde{H}_1(\alpha)\, e^{-k_0 u_1 (z-\tau)}, z \geq \tau \\ \tilde{H}_2(\alpha)\, e^{-k_0 u_2 (z-\tau)}, z \leq \tau \end{cases} \tag{A-6}$$

where

$$u_1 = (\alpha^2 - n_1^2)^{1/2},\ \mathrm{Re}\, u_1 > 0 \tag{A-7}$$

$$u_2 = (\alpha^2 - n_2^2)^{1/2} \tag{A-8}$$

Applying the continuity of E_r and E_φ at $z = \tau$ implies that $\tilde{H}_z$ and $\frac{\partial \tilde{E}_z}{\partial z}$ are continuous there, whence (A-5) and (A-6) become

$$\tilde{E}_z(\alpha,z) = \begin{cases} \tilde{E}_z(\alpha)\, e^{-k_0 u_1 (z-\tau)}, z \geq \tau \\ -\tilde{E}_z(\alpha) \left[\frac{u_1}{u_2}\right] \frac{\cosh(k_0 u_2 z)}{\sinh(k_0 u_2 \tau)}, z \leq \tau \end{cases} \tag{A-9}$$

$$\tilde{H}_z(\alpha,z) = \begin{cases} \tilde{H}_z(\alpha)\, e^{-k_0 u_1 (z-\tau)}, z \geq \tau \\ \tilde{H}_z(\alpha) \frac{\sinh(k_0 u_2 z)}{\sinh(k_0 u_2 \tau)}, z \leq \tau \end{cases} \tag{A-10}$$

We need now to apply the source conditions at $z = \tau$ to determine the coefficient functions $\tilde{E}_z(\alpha)$ and $\tilde{H}_z(\alpha)$.

To apply the source condition for $\tilde{E}_z(\alpha)$, recall that if ρ_s and $\bar{J}_s$ are the surface charge and current densities, respectively, in the $z = \tau$ plane, then $\rho_s = \frac{i}{\omega} \nabla_t \cdot \bar{J}_s$ and $n_1^2 E_z(r,\varphi,\tau_+) - n_2^2 E_z(r,\varphi,\tau_-) = \rho_s / \varepsilon_0$.

Substituting the former expression into the latter and using (2.2-1) to give

$$\bar{J}_s = I\, e^{-in\varphi}\delta(\tau - \tau_0)\hat{\varphi} \tag{A-11}$$

$$n_1^2 E_z(\tau,\varphi,\tau_+) - n_2^2 E_z(\tau,\varphi,\tau_-) = \left[\frac{n}{\varepsilon_0\omega}\right] I\, e^{in\varphi}\,\frac{\delta(\tau-\tau_0)}{\tau} \tag{A-12}$$

Canceling $e^{-in\varphi}$, multiply on both sides by $k_0^2\, J_n(k_0\alpha\tau)\tau\, d\tau$, and integrating over $[0,\infty]$ in (A-12), one has

$$n_1^2\tilde{E}_z(\alpha,\tau_+) - n_2^2\tilde{E}_z(\alpha,\tau_-) = nk_0\zeta_0 I J_n(\alpha k_0\tau_0) \tag{A-13}$$

Using (A-9) with (A-13) yields $\tilde{E}_z(\alpha)$ as given in (2.1-10).

To apply the source condition for $\tilde{H}_z(\alpha)$, recall that if $\bar{J}_s$ is the surface current density in the $z = \tau$ plane, then $\bar{H}_t(\tau,\varphi,\tau_+) - \bar{H}_t(\tau,\varphi,\tau_-) = \hat{z}\times\bar{J}_s$, where the subscript "t" denotes field components transverse to the z-direction. Using equation (A-11) for $\bar{J}_s$ and applying $(\nabla_t\cdot)$ on both sides of the expression above gives

$$\frac{\partial H_z}{\partial z}(\tau,\varphi,\tau_+) - \frac{\partial H_z}{\partial z}(\tau,\varphi,\tau_-)$$

$$= \frac{-Ie^{-in\varphi}}{\tau}\left\{\delta(\tau-\tau_0) + \tau\,\delta'(\tau-\tau_0)\right\} \tag{A-14}$$

Cancelling $e^{-in\varphi}$, multiplying both sides by $k_0^2\, J_n(k_0\alpha\tau)\,\tau d\tau$, and integrating over $[0,\infty]$ in (A-14) gives

$$\frac{\partial}{\partial z}\tilde{H}_z(\alpha,\tau_+) - \frac{\partial}{\partial z}\tilde{H}_z(\alpha,\tau_-) = \alpha k_0^3\, I\tau_0\, J_n'(\alpha k_0\tau_0) \tag{A-15}$$

Using (A-10) with (A-15) yields $\tilde{H}_z(\alpha)$ as given in (2.1-11).